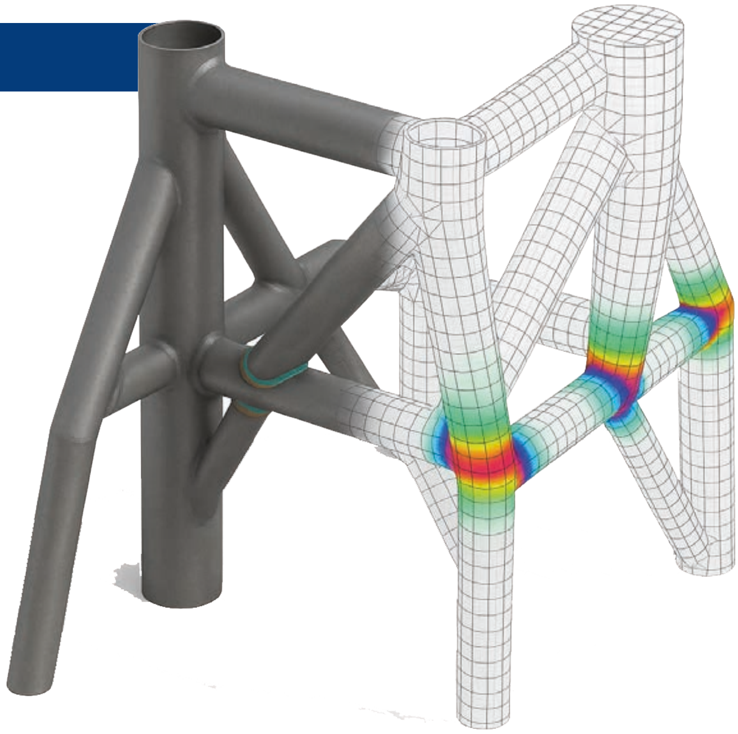

Fatigue strength assessment of large welded K-nodes in the offshore industry: a comparison of approaches using MAGNA FEMFAT software

by Alberto Visentin and Giovanni Meneghetti
Department of Industrial Engineering, University of Padua

When it comes to the fatigue design and durability assessment of modern welded engineering structures, mechanical engineers are faced with the dual challenge of large-scale complex geometries and constant and time-varying real-world loads. The most common approach is to use methods based on nominal stresses, as set out in international standards and recommendations. These approaches allow analysts to calculate the nominal linear-elastic stresses acting on a welded component using simple solid mechanics formulas, regardless of the weld's geometry. The calculated stress must then be compared with the fatigue strength of a suitably classified structural detail, depending on its geometry and loading conditions.

Standards provide a wide range of references for fatigue designs, which are commonly known as "FAT" classes. These are valid for the most common welded components encountered in engineering practice. However, the standards do not always provide the appropriate classified details for complex geometries and multi-axial loading conditions. Finite element (FE)-assisted *approaches*, such as the hot-spot and *notch stress* methods, have been shown to reliably complement the popular nominal stress method. Nevertheless, in some circumstances, advanced methods for the fatigue design of welded structures, such as the *notch stress approach*, may require the following:

1. time-consuming pre-processing procedures to accurately model the detailed geometry of welds.
2. significant computing resources to solve FE models with locally refined meshes near the welds; and
3. manual routines to post-process FE stress results in order to evaluate the fatigue strength of welds.

With this in mind, it is clear that evaluating the fatigue strength of large welded structures can be challenging in terms of time, computing resources and the qualified personnel required for finite element analysis. These challenges are commonly encountered in sectors such as amusement park structures, automotive design, offshore structures, mining and earth-moving, and agriculture vehicles and equipment. This prompts companies to look for simplified analysis techniques that provide reliable results quickly.

In this context, the value of commercial fatigue analysis tools lies in their ability to automate the application of well-established methods, thereby reducing the time and effort required for post-processing FE-calculated stresses and performing fatigue durability estimates.

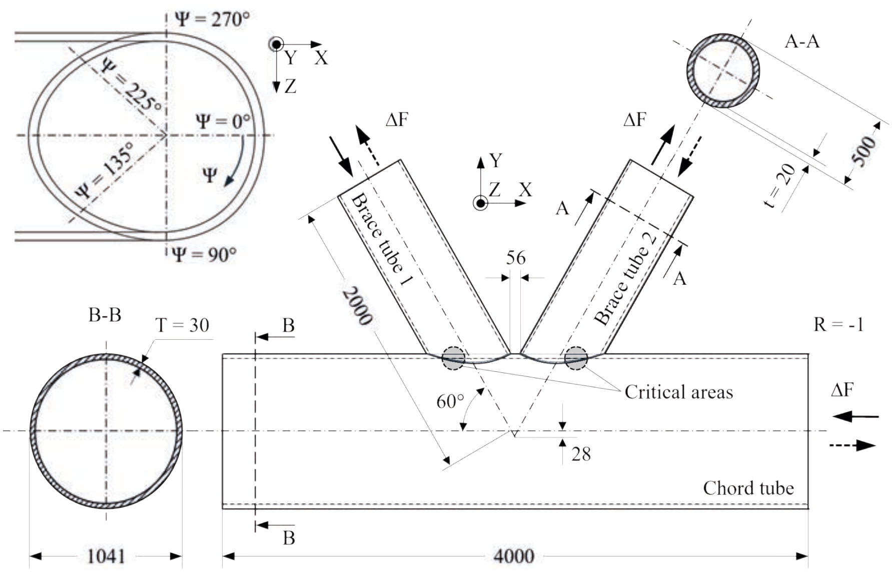

Fig. 1. Geometry of welded K-nodes. The dimensions shown are in millimetres.

Introduction

This study used the MAGNA FEMFAT commercial software to assess the fatigue strength of large welded K-nodes, which are commonly used on small offshore platforms. Firstly, three different FE models of a real large K-node were developed in Ansys Mechanical using 3D *shell* and 3D *solid* finite elements. The FEMFAT fatigue analysis tool was then used to post-process the extracted stress results from the Ansys finite element analyses in order to estimate fatigue durability. Three fatigue analysis approaches implemented in FEMFAT (the *Shell* WELD approach, the *Solid*WELD approach, and the R1MS approach) were then compared. A set of experimental data from the literature relevant to the fatigue strength of the welded K-nodes under investigation was considered and re-evaluated. Finally, the number of cycles to crack initiation in experimental fatigue failures was compared with the fatigue life estimates made using the S-N fatigue design curves implemented in FEMFAT.

Large K-joints for the offshore industry

C. M. Sonsino [1–3] investigated the fatigue strength of large, welded K-joints made of E355 fine-grained structural steel under normalized conditions ($\sigma_{Y0.2} \geq 355MPa$ and $\sigma_U \geq 470MPa$ in [1]). The welded specimen consisted of two diagonal tubular braces, each with a diameter of 500mm and a thickness of 20mm. The braces were joined to a chord tube with a diameter of 1,041mm, a thickness of 30mm, and a length of 4,000mm at a 60-degree angle of incidence (see Fig.1). A full-penetration welded connection was achieved between the ends of the brace tube and its surface using conventional multi-layer welding. During the joining process, a 56mm gap was generated between the two braces (see [1]).

Experimental fatigue tests were performed with constant and variable amplitude loads using a dedicated test rig equipped with a servo-hydraulic actuator with a maximum load capacity of 2,500kN. The actuator was connected to the chord, and the applied horizontal load was transmitted to the braces via longitudinal bars [3]. As a result, the braces tubes experienced fully reversed axial loads, while the chord tube experienced a unidirectional tensile-compressive axial load with a load ratio of $R = -1$ [1–3].

A total of eight specimens were tested for fatigue resistance in an artificially generated seawater environment (see Table 1). The seawater was continuously aerated and circulated around the welds, and no corrosion protection was applied [1]. Three specimens underwent fatigue testing with constant amplitude (CA) loads and five specimens underwent fatigue testing with variable amplitude (VA) loads using a standard relative load spectrum (or stress amplitude) derived from wave loads in the North Sea [1–3]. Fig. 2 shows this spectrum, characterized by a spectrum factor of 1.0 (i.e. linear in a log-linear diagram) and a length of $L_s = 5{\cdot}10^6$ cycles. According to the COLOS (Common Load Sequence) standard [1], this corresponds to an operating time of one year.

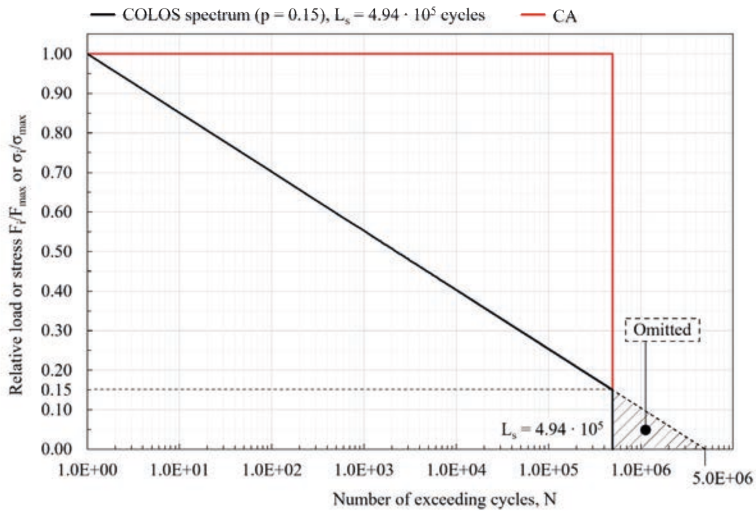

Fig. 2. In accordance with the COLOS (Common Load Sequence), the standard North Sea wave load spectrum is used for load configurations with variable amplitude (VA) [3].

Specimen No.	Load range ΔF_{max} [MN] *	Stress amplitude scale factor f_s ^	Crack initiation N_{init} [cycles]	Breakthrough N_{bt} [cycles]	Site of crack initiation	
					Ψ (°)	Brace
6, CA	1.50	1.07	$1.60 \cdot 10^5$	$3.95 \cdot 10^5$	90	1
7a, CA	1.00	0.71	$6.00 \cdot 10^5$	$1.92 \cdot 10^6$	105	1
7b, CA	1.00	0.71	$8.05 \cdot 10^5$	$1.92 \cdot 10^6$	270	1
1, VA	3.00	2.14	$5.93 \cdot 10^5$	$2.22 \cdot 10^6$	90	2
10, VA	3.00	2.14	$8.00 \cdot 10^5$	$3.96 \cdot 10^6$	225	1
13, VA	1.70	1.21	$7.42 \cdot 10^5$	$1.46 \cdot 10^7$	120	1
3, VA	2.00	1.43	$2.82 \cdot 10^6$	$1.29 \cdot 10^7$	120, 135	1,2
2, VA	2.00	1.43	$1.20 \cdot 10^5$	$6.30 \cdot 10^6$	90	1

** Maximum load range applied in experimental fatigue tests.*
^ Stress amplitude scaling factor, according to Eq. (2), is used to linearly scale the stress amplitude results calculated using FEM.

Table 1. Relevant experimental fatigue results for K-nodes tested under constant and variable amplitude loading.

As stated in [1], all stress amplitudes below 15% were omitted to achieve reasonable test periods. Moreover, it is assumed that fatigue damage is primarily caused by high stress amplitudes while lower stresses do not significantly contribute to the damage process [1]. Modifying the original spectrum produced a reduced spectrum with a spectrum length of $L_s = 4.94{\cdot}10^5$ cycles and a p-factor of 0.15. Here, p is the ratio of the minimum to maximum stress amplitude in the spectrum.

Fatigue loads were applied repeatedly until fatigue cracks initiated at the weld toe of the chord near the saddle points of braces 1 and 2 (see Fig. 1), at an angular position of approximately 0–45° from the saddle point (i.e. $\Psi = 90 \div 135°$, see Table 1). The fatigue life at crack initiation was defined by assuming a technical crack with a depth of 1mm and a surface extension of $2l = 20mm$, as measured using potential-drop techniques. Subsequently, the fatigue cracks propagated through the chord tube, and the total fatigue life was defined as the number of cycles to breakthrough (failure) [1–3].

FE fatigue strength assessment using shell and solid FE models

The fatigue strength of the welded K-node in Fig. 1 was investigated numerically using the MAGNA FEMFAT fatigue analysis tool. The following approaches were considered for comparison purposes:

(i) The FEMFAT Shell WELD approach requires an FE model solved using linear or quadratic shell finite elements as input. This approach does not model the detailed geometry of the welds and recommends a maximum element edge length of twice the plate thickness to provide sufficient mesh refinement for calculating structural stresses. Nodes and elements that share the seam line between the joining plates — referred as *"weld nodes"* and *"weld elements"* — can be saved in *named selections* so that FEMFAT can easily locate them.

(ii) The FEMFAT *Solid*WELD approach requires an FE model solved using quadratic *solid* finite elements. The detailed geometry of the welds must be included in the model. Rather than modelling the weld toes and weld roots with rounded edges and roots, they should be modelled as sharp V-notches. The FE mesh should be locally refined around the profile of the welds, providing at least three elements across the sheet metal thickness. This should be done while ensuring that the maximum size of the finite elements is $1 \div 2mm$. When creating the input FE model, the nodes belonging to the weld toe and weld root should be stored in *named selections* according to the nomenclature set out in the FEMFAT guidelines.

(iii) The FEMFAT R1MS approach requires am FE model that has been solved and generated using quadratic solid finite elements. The model must include the detailed geometry of the welds. Additionally, a notch radius should be introduced at the weld toe and weld root. According to the FEMFAT guidelines, the notch radius at the weld toe should be 1mm for thicknesses greater than 5mm. On the other hand, the notch radius should be equal to 0.05mm at the weld toe for thicknesses lower than 5mm. A notch radius equal to 0.05mm is always recommended for crack-like notches (e.g. at the weld root). To achieve convergence of the local stress field, the local element size should be approximately one-tenth of the notch radius.

Ansys Mechanical FE software was used to generate the three input models of the welded K-node, as shown in Fig. 3, in accordance with the modelling guidelines for the FEMFAT software. More specifically:

(i) An FE *shell* model of the welded K-node was developed by modelling the intermediate surfaces of the chord and brace tubes. Half of the joint was modelled using the XY symmetry plane (see Fig. 1a). The geometry of the weld beads was not included. Table 2 shows that a free 8-node FE *shell* mesh (SHELL 281 from the Ansys FE library) was generated, with an element size of $2t = 40mm$ overall. Here, t represents the minimum sheet metal thickness in the model (i.e. the thickness of the braces elements). Loads and constraints were applied as shown in Fig. 3a to replicate the loading conditions in the experimental fatigue tests. The time required to solve the linear elastic FE analysis in Ansys Mechanical was four seconds (see Table 2). The resultant Ansys CDB file (approximately 2.7MB), containing the finite element mesh data (i.e. nodes and elements), and the RST file (approximately 7.2MB), containing the stress amplitude results, were extracted for import into FEMFAT.

(ii) A *solid* volume-based FE model of the welded K-node was developed by modelling only half of the geometry, since it is symmetrical with respect to the XY plane (see Fig. 3b). The model included detailed, realistic, full-penetration weld geometry, with the brace and chord-side weld toes modelled as sharp, V-shaped notches. In accordance with the FEMFAT *Solid*WELD meshing guidelines, a free mesh comprising 10-node tetrahedral finite elements (SOLID 187 from the Ansys FE library) was generated with a local element size of 1mm around the weld toes. The size was specified in the weld bead region and extended approximately 20mm from the weld toe lines. Outside the locally refined mesh region, the size of the tetrahedral elements was gradually increased to 20mm (equivalent to the brace thickness, t) in order to decrease the mesh density as much as possible and generate only one element in the thickness of the brace tube. Finally, all the *Solid*WELD nodes (i.e. the nodes located at the weld toes) were collected into a named selection called *"FemfatSolidWeld_1_toe_y-joint_30p0"*, in accordance with the FEMFAT *Solid*WELD naming guidelines. Here, *"toe"* specifies the type of weld edge, and *"30p0"* refers to the maximum thickness between the welded members of the K-node (i.e. the chord tube thickness). Solving the linear elastic FE analysis in Ansys Mechanical took approximately 11

FE model	Adopted finite element type (code in Ansys FE library)	Global FE size [mm]	Local FE size [mm]	Number of DOF*	FEA solution time [s] ^
Figure 3a	8-node shell (SHELL 281)	40	40.0	$8.30 \cdot 10^4$	4
Figure 3b	10-node tetrahedral (SOLID 187)	20	1.0	$1.75 \cdot 10^7$	644 ~ 11 minutes
Figure 3c	10-node tetrahedral (SOLID 187)	20	0.1	$1.02 \cdot 10^8$	$1.2 \cdot 10^4$ ~ 3.33 hours

^ Machine hardware: CPU: Intel Core i9-10900X @ 3.70GHz; RAM: 128GB; GPU: NVIDIA T400, 4GB.
** For 10-node tetrahedral elements, there are three degrees of freedom per node; for 8-node shell elements, there are five degrees of freedom per node.*

Table 2. Finite element types and sizes used to generate input FE models in Ansys Mechanical software.

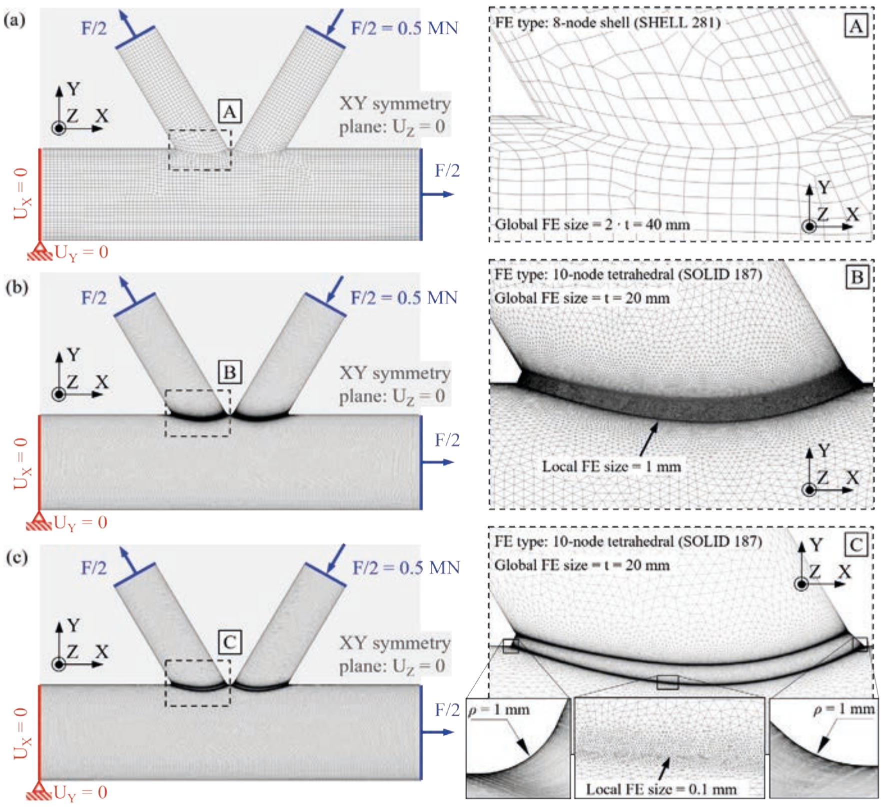

Fig. 3. The K-node FE models generated in Ansys Mechanical and adopted for fatigue strength analysis using MAGNA FEMFAT software. (a) A detail of the 8-node shell FE model using the FEMFAT Shell WELD approach. (b) A detail of the 10-node tetrahedral solid FE model with modelled weld beads using the FEMFAT SolidWELD approach. (c) A detail of the 10-node tetrahedral solid FE model with modelled weld beads and a $\rho = 1mm$ notch radius at the weld toes using the R1MS approach.

minutes (see Table 2). The resulting Ansys CDB file (approximately 1.4GB), which contains the FE mesh data (i.e. nodes and elements), and the RST file (approximately 3GB), which contains the stress amplitude results, were extracted for import into FEMFAT.

(iii) A *solid* volume-based FE model of the welded K-node was developed by modelling only half of the geometry, as it is symmetric with respect to the XY plane (see Fig. 3c). As in the previous case (ii), the model included the detailed geometry of the full-penetration weld beads. Additionally, a $\rho = 1mm$ notch radius was introduced at the weld toes for both the brace and the chord members. Free meshing with 10-node, tetrahedral SOLID 187 fine elements (from the Ansys FE library) was generated. A local dimension of 0.1mm (i.e. $\rho/10$) was assigned to the notch faces extending to the weld toe (see Fig. 3c). Then, the free meshing algorithm in Ansys Mechanical was used to progressively increase the size of the finite elements away from the notch regions. To ensure the presence of at least one element through the thickness of the brace member, t, a 20mm element size was chosen. According to the FEMFAT R1MS naming guidelines, all FE nodes along the weld toes were collected in a *named selection* called *"C200"*. Solving the linear elastic FE analysis in Ansys Mechanical took approximately 3.33 hours (see Table 2). The resulting Ansys CDB file containing the FE mesh data (i.e. nodes and elements) was approximately 8.2GB. The RST file, which contains the stress amplitude results, was approximately 15GB. Both files were extracted and imported into FEMFAT for the fatigue strength analysis.

The input models (i)–(iii) were defined in Ansys Mechanical, exported as CDB files containing the FE mesh entities (i.e. nodes and elements), and imported into the FEMFAT fatigue analysis tool.

For the *shell* input model of the FEMFAT *Shell* WELD analysis (see Fig. 3a), the automated routine in the FEMFAT *Visualizer* that identifies seam lines between the chord and braces tubes (i.e. the weld edges) was used successfully. Two reference joint categories were identified in the available FEMFAT structural steel joint detail databases: (1) the "T90-JOINT (FAT80/100)" weld detail from the *Eurocode 3/9* database (Fig. 4a), and (2) the "TJOINT – HV Seam" weld detail from the *ECS standard* database (Fig. 4b). Both details pertain to a one-sided, full-penetration weld in a T-joint with a 90-degree inclination angle between the main and stiffener plates (see Fig. 4). This represents the welded connection between the chord and braces locally. Finally, the same joint detail was assigned to each node along the identified *weld edges*.

No pre-processing operations were required to define the welded connection between the chord and the braces in the input solid model used for the FEMFAT *Solid*WELD analysis (see Fig. 3b). This is because the model already displays the detailed weld bead geometry and the nodes along the brace-side and chord-side weld toes are automatically detected by FEMFAT during geometry import. These nodes were collected in the *"FemfatSolidWeld_1_toe_y-joint_30p0" named selection*. Similarly, in the case of the *solid* model for the FEMFAT R1MS analysis (see Fig. 3c), the weld nodes belonging to the 1mm-notch faces were automatically detected and collected by FEMFAT in the *"C200" named selection.* This eliminated the need for additional manual pre-processing activities.

All FEMFAT analyses have been performed using the FEMFAT *ChannelMAX* module. This enables the FE analyst to:

- import the stress amplitude results extracted from the Ansys Mechanical FE software and assign them to one or more *Channels* based on the number of load steps stored in the FE results file;
- import or define a time-history of applied stresses in terms of normalized stress amplitude (e.g. σ/σ_{max}); and
- specify a multiplication factor for the imported stresses, if required.

FEMFAT Approach	WELD Database WELD Detail	WELD Method	Miner Formulation	Number of Analysed Nodes	FEMFAT Solution Time ^	
					CA*	VA**
Shell WELD	Eurocode 3/9 database T90JOINT - FAT80/100	*Eurocode 3/9*	Eurocode 3/9 (= Miner Modified)	86	2 seconds	3 minutes
Shell WELD	ECS database TJOINT - HV Seam	*FEMFAT 4.7*	Miner Modified	86	2 seconds	3 minutes
SolidWELD	-	*FEMFAT 4.7*	Miner Modified	7,016	60 seconds	60 minutes
R1MS	-	*FEMFAT 4.7*	Miner Elementary	803,344	15 minutes	20 hours

^ Adopted hardware: CPU: Intel Core i9-10900X @ 3.70GHz; RAM: 128GB; GPU: NVIDIA T400, 4 GB.
** Solution time required for one FEMFAT analysis of Constant Amplitude (CA) loads.*
*** Solution time required for one FEMFAT analysis of Variable Amplitude (VA) loads.*

Table 3. Summary of fatigue strength analyses performed using FEMFAT software.

In Ansys Mechanical, it is worth noting that the three forces acting on the braces and chord of the K-node (see Fig. 1) were applied in a single load step. Therefore, a single *Channel* and load time-history of the applied stress amplitudes, taking the total applied load into account, is sufficient (see Fig. 3).

The following procedures were adopted for of the models shows in Fig. 3:

- For constant amplitude (CA) fatigue loads, the Ansys RST results file was imported using a single FEMFAT *Channel*. A single load cycle acting on the K-node was simulated by defining a fully reversed normalized *triangular* load history ($R=-1$) using the Time Histories in FEMFAT.

For variable amplitude (VA) fatigue loads, the Ansys RST results file was imported using a single FEMFAT *Channel*. The COLOS stress spectrum was then converted into a load history with a load ratio of $R=-1$ a spectrum length of $L_s=4.94{\cdot}10^5$ cycles (1 point/cycle) and $p=0.15$ (see Fig. 2). This was done in accordance with the experimental testing framework. An RPC file of the time-history was then generated and imported in accordance with the FEMFAT guidelines.

The *material generator* in FEMFAT was used to quickly define all the necessary material data, which is specified as follows:

- Ultimate strength: 515MPa;
- Yield strength: 362MPa;
- Young's modulus: 206000N/mm^2; and
- Elastic poisson's Ratio: 0.28

This is in accordance with the data reported by the original author [1].

The material properties were applied to all the model nodes in the *Node Characteristics* section. For the FEMFAT R1MS analysis, the *"WELD-ASTM-50_toe_r=1_mm_ECS.ffd"* material database was imported in accordance with the FEMFAT R1MS guidelines. The relevant material properties were then applied to the nodes in the *"C200"* group in the *Node Characteristics* section.

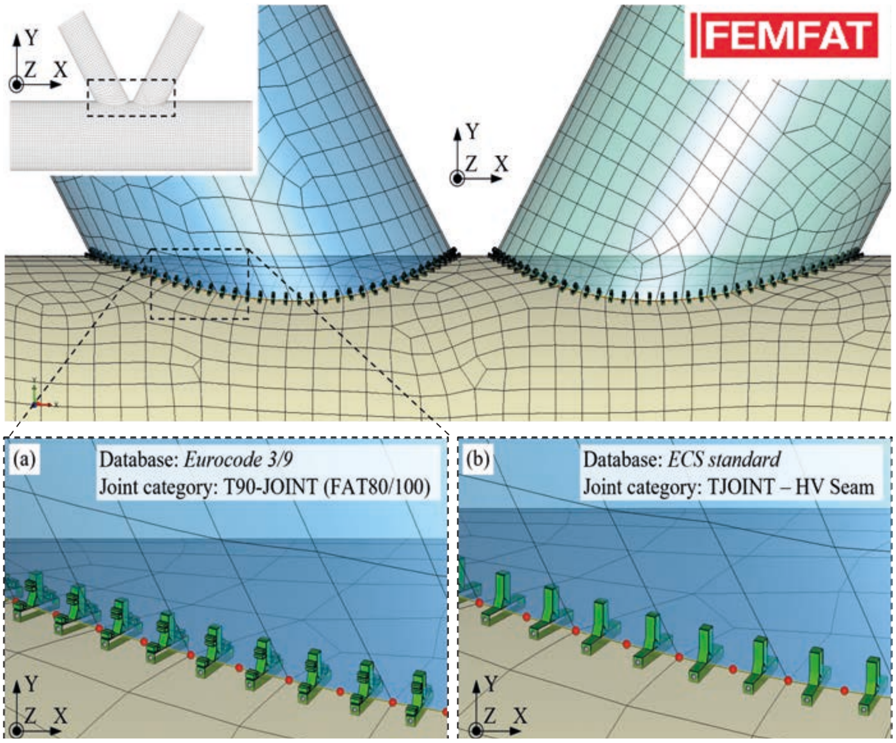

Fig. 4. Definitions of weld edges and the associated joint categories in FEMFAT Visualizer, as defined in (a) the Eurocode 3/9 database and (b) the ECS database.

A total of 32 FEMFAT analyses were conducted based on the experimental data presented in Table 1 using four types of FEMFAT fatigue strength analysis. Table 3 shows the main parameters adopted for each analysis, alongside the corresponding solution time. More specifically, there were:

(a) Eight fatigue analyses were performed using the FEMFAT *Shell* WELD approach in conjunction with the *Eurocode 3/9* analysis method (see Table 3). The *shell* FE model in Fig. 3a was used as input. The WELD setting, which uses the *Eurocode 3/9* method, was enabled in FEMFAT. The *"Signed Mises (Sign from Sigma_perpendicular)"* equivalent stress was selected to use the available von Mises-based formulation and combine the notch stress amplitude components into an equivalent notch stress amplitude at each analysed *weld node* according to the following expression [4]:

$$\sigma_{eq,VM} = sign(\sigma_{a\perp})\sqrt{\sigma_{a\perp}{}^2 + \sigma_{a\parallel}{}^2 + \sigma_{a\perp} \cdot \sigma_{a\parallel} + 3 \cdot \tau_a{}^2}$$

Equation (1)

Where:

- $\sigma_{a\perp}$ is the amplitude of the normal stress at the notch that acts orthogonally to the *weld edge;*
- $\sigma_{a\parallel}$ is the amplitude of the normal stress at the notch that runs parallel to the *weld edge;*
- τ_a is the amplitude of the tangential stress at the notch.

For a complete overview of the theoretical background, please refer to the FEMFAT guidelines [4].

The *Automatic Stress Correction* function in the WELD Stress settings was enabled, and the *Stress Interpolation* Parameters $A = B = 0.280$ and $C = 0.000$ were adopted. This ensured that the local stresses were extracted 14mm from the junction line between the chord shell plate and the brace *shell* plate. This corresponds to the approximate position of the *weld* toe of the chord tube.

Finally, the *Statistical General Factor* was used to set a 50% probability of survival, which was adopted for fatigue strength estimates. No other *Influence Factors* were considered in the analysis. The *Analysis Target* was set to *Damage*, and the Miner formulation of *Eurocode 3/9* was specified for the damage calculation. The default cutoff limit of 10^8 cycles was maintained for the S-N curve.

As stated in the FEMFAT guidelines, it is important to note that the *Eurocode 3/9* formulation aligns with the *Miner Modified* formulation. A 50% probability of survival was specified in the *Global Parameters*. No additional *Analysis Parameters* were required. A fatigue strength assessment was conducted on the *86 weld nodes* (i.e. the nodes along the identified *weld edges*) as reported in Table 3. This table was previously compiled in a dedicated group in FEMFAT. Each *Shell* WELD analysis using the *Eurocode 3/9* method took two seconds to solve for the CA loads and three minutes for the VA loads.

(b) A total of eight fatigue analyses were performed using the FEMFAT *Shell* WELD approach combined with the *FEMFAT 4.7* method (see Table 3). As in case (a) above, the FE *shell* model in Fig. 3a was used as input. The WELD setting was enabled using the *FEMFAT 4.7* analysis method. The WELD settings previously described in (a) were adopted here as well. The *Statistical General Factor* was enabled to account for a 50% probability of survival in fatigue strength calculations. The *Analysis Target* was set to *Damage*, and the *Miner Modified* formulation was specified for the damage calculation. A *probability of survival* was specified in the *Global Parameters.* Finally, the *Absolute Stress Limit* for the WELD in the *Analysis Filter* was set to 0N/mm^2.

This allowed FEMFAT to consider all stress amplitudes during the damage analysis rather than filtering out the low ones. It is important to note that FEMFAT did not use this *filter analysis parameter* in the *Eurocode 3/9* method (see point (a) above). The fatigue strength evaluation was conducted on 86 *weld nodes* that were previously collected in a dedicated FEMFAT *group* (see Table 3). Each *Shell* WELD analysis combined with the *FEMFAT 4.7* method took two seconds for the CA load cases and three minutes for the VA load cases.

(c) A total of eight fatigue analyses were performed using the FEMFAT *Solid*WELD approach in conjunction with *FEMFAT 4.7* method for post-processing the linear elastic stresses (see Table 3). The solid FE model shown in Fig. 3b was used as input data. The WELD setting was enabled in FEMFAT using the *FEMFAT 4.7* analysis method. Equivalent stress *("Signed Mises-Stress 1, sign from maximum principal stress)* was selected to analyse the *Solid*WELD nodes. The von Mises-based formulation was used to combine the notch stress amplitude components at each analysed node according to Eq. (1). For a complete overview of the theoretical background and other available formulations for equivalent peak stress at *Solid*WELD nodes, please refer to the FEMFAT guidelines.

The *Statistical General Factor* was used to set a 50% probability of survival, and this was taken into account in the fatigue strength calculations. No other *Influence Factors* were considered in the analysis. The *Analysis Target* was set to *Damage* and the *Miner Modified* formulation was specified for the damage calculation. The von Mises equivalent stress method and a 50% probability of survival were assigned in the *Global Parameters*.

As *Solid*WELD nodes are part of the base material, the *Absolute Stress Limit for Base Material* in the Analysis Filter was set to 0N/mm^2 to deactivate the low stress amplitude filter during damage analysis. A fatigue strength assessment was conducted on 1,056 *Solid*WELD nodes (i.e. nodes located at the brace and chord weld toes), as shown in Table 3. These nodes were previously isolated in the *"FemfatSolidWeld 1toe y-joint 30p0"* named selection in Ansys Mechanical and then imported into FEMFAT. Each *Solid*WELD analysis combined with the *FEMFAT 4.7* method required 60 seconds of solution time for the CA load cases and 60 minutes for the VA load cases.

(d) A total of eight fatigue analyses were performed using both the FEMFAT R1MS approach and the *FEMFAT 4.7* method (see Table 3). The *solid* FE model shown in Fig. 3c was used as input data. The WELD setting was enabled in the settings for the *FEMFAT 4.7* analysis method. As in previous cases (a)–(c), the *Statistical General Factor* was included to relate the fatigue strength estimates to 50% probability of survival. No additional *Influence Factors* were considered in the analysis. In line with previous analyses (a)–(c), the *Analysis Target* was set to *Damage* and the *Miner Elementary* formulation was specified for the damage calculation. This ensures that the slope of the S-N curve adopted in calculations extends beyond the cut-off limit (see Fig. 11).

The von Mises equivalent stress method and a *50% probability of survival* was specified as the *Global Parameters*. Since FEMFAT considers the target nodes belonging to the notch faces to be part of the base material, the *Absolute Stress Limit* for Base Material in the *Analysis Filter* was set to $0N/mm^2$ to prevent filtering at low stress amplitudes during the damage analysis.

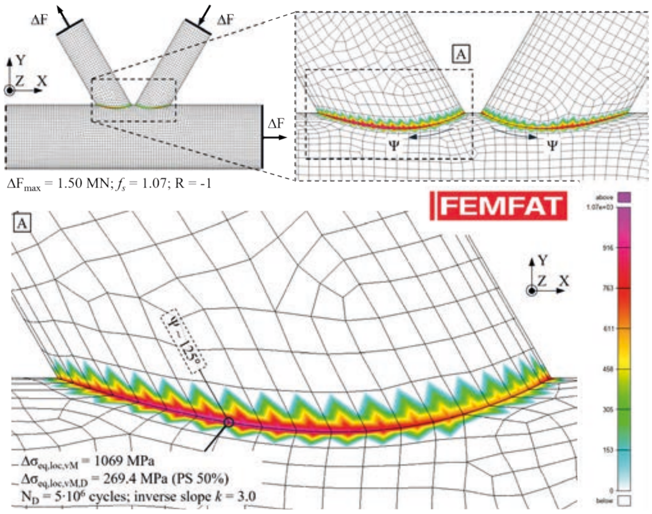

Fig. 5. The Von Mises equivalent stress range for specimen “6, CA” (see Table 1) using the FEMFAT Shell WELD approach in conjunction with the Eurocode 3/9 WELD method.

Fatigue strength evaluations were conducted on 803,344 nodes belonging to the 1mm notch faces (see Table 3). These nodes were initially collected in the *“C200” named selection* within Ansys Mechanical and then imported into FEMFAT. Each R1MS analysis combined with the *FEMFAT 4.7* method took 15 minutes to solve for the CA load cases and approximately 20 hours for VA load cases.

Figs. 5–8 show the results of FEMFAT analyses (a)–(d), calculated in terms of equivalent von Mises stress range ($\Delta\sigma_{eq,loc,vM}$) at the FE nodes analysed. They are represented graphically on a mesh view of the model via *contour plots* generated by the FEMFAT *Visualizer* tool. This example relates to the “6, CA” welded specimen in Table 1.

Fig. 5 shows the *contour plot* of the von Mises equivalent stress range, which was calculated along the *weld edges* and analysed using the FEMFAT *Shell* WELD approach in combination with the *Eurocode 3/9* method. The most critical point is located at $\Psi \sim 125°$ on the *weld edge* between the chord tube and brace tube 1. Furthermore, von Mises equivalent stress range values comparable to the maximum value within a 5% deviation are obtained along the *weld edge* of brace tubes 1 and 2, in regions extending approximately from $\Psi = 90°$ to $\Psi = 140°$ and $\Psi = 90°$ to $\Psi = 120°$, respectively. There is good agreement between the resulting critical points (Fig. 5) and the crack initiation sites observed during the experimental tests. According to references [1–3] (see Table 1), these sites range between $\Psi = 90°$ and $\Psi = 135°$.

Fig. 6 shows the *contour plot* of the von Mises equivalent stress *amplitude* calculated along the *weld edges* using a combination of the FEMFAT *Shell* WELD approach and *FEMFAT 4.7* analysis method. The most critical point is located at $\Psi \sim 125°$ on the weld edge of brace tube 1. This is consistent with the result obtained using the *Eurocode 3/9* method (see Fig. 5). In addition, von Mises equivalent stress amplitude values comparable to the maximum value within a 5% deviation are obtained along the *weld edge* of brace tube 1 in a region extending approximately between $\Psi = 100°$ and $\Psi = 150°$, as well as along the *weld edge* of brace tube 2 in a region extending between $\Psi = 100°$ and $\Psi = 120°$. As in Fig. 5, there is a good agreement between the resultant critical points (Fig. 6) and the experimental crack initiation sites, which range between $\Psi = 90°$ and $\Psi = 135°$ [1–3] (see Table 1).

Fig. 7 shows the *contour plot* of the von Mises equivalent stress *amplitude*, as calculated using the FEMFAT *Solid*WELD approach and the *FEMFAT 4.7* analysis method at the brace- and chord-side weld toes. The node with the maximum von Mises equivalent stress *amplitude* value (i.e. the most critical point) is located at $\Psi \sim 110°$ along the chord-side weld toe, between the chord tube and brace tube 1. Comparable von Mises equivalent stress amplitude values within a 5% deviation from the maximum value are obtained along the chord-side weld toe of brace tube 1, extending from approximately $\Psi = 90°$ to $\Psi = 135°$, as well as

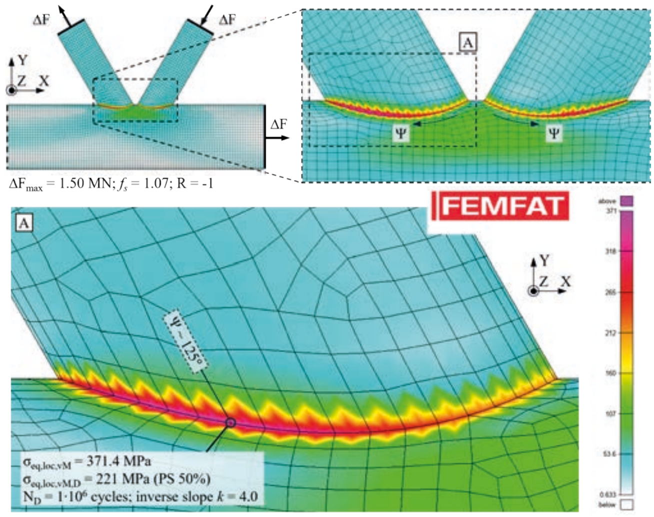

Fig. 6. The Von Mises equivalent stress amplitude for specimen “6, CA” (see Table 1) using the FEMFAT Shell WELD approach combined with the FEMFAT 4.7 WELD method.

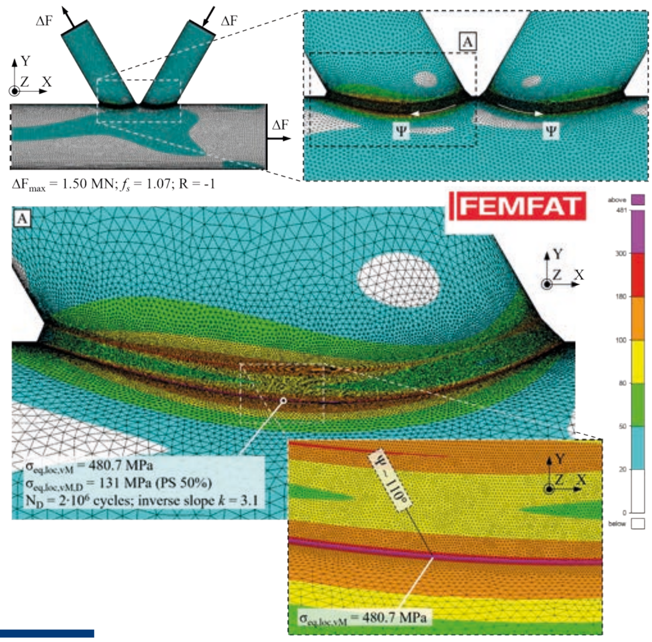

Fig. 7. The Von Mises equivalent stress amplitude results for specimen “6, CA” using the FEMFAT SolidWELD approach in conjunction with the FEMFAT 4.7 WELD method.

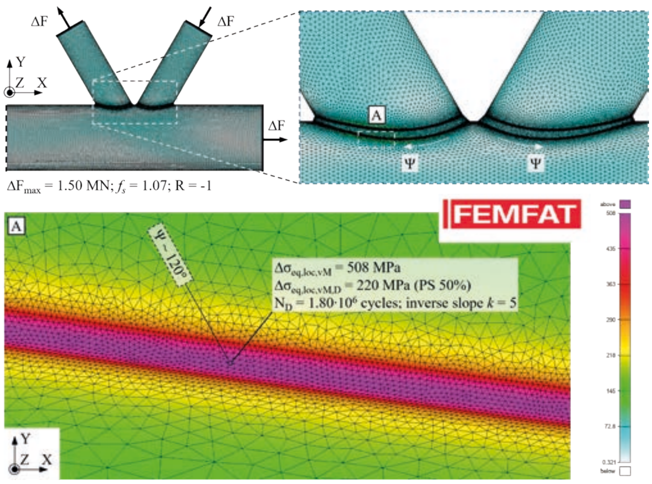

Fig. 8. The Von Mises equivalent stress range for specimen "6, CA" (see Table 1) using a combination of the FEMFAT R1MS approach and the FEMFAT 4.7 WELD method.

along the chord-side weld toe of brace tube 2 in a region extending from approximately $\Psi = 90°$ to $\Psi = 120°$. There is very good agreement between the estimated critical points (Fig. 7) and the experimental crack initiation sites, which range between $\Psi = 90°$ and $\Psi = 135°$ [1–3] (see Table 1).

Finally, Fig. 8 shows the von Mises equivalent stress *range contour plot*, which was calculated using the FEMFAT R1MS and approach and *FEMFAT 4.7* analysis method. The analysis was performed at the brace-side and chord-side weld toes. The area in which the maximum von Mises equivalent stress range value is obtained is the most critical point. This point is located at $\Psi \sim 120°$ on the chord-side weld toe, between the chord tube and brace tube 1. Similar von Mises equivalent stress *range* values, deviating by no more than 5% from the maximum value, are at the chord-side weld toe of brace tube 1, within a region extending from approximately $\Psi = 70°$ to $\Psi = 150°$. The same is true for the chord-side weld toe of brace tube 2, within a region extending from approximately $\Psi = 100°$ to $\Psi = 150°$. Once again, there is excellent agreement between the estimated critical points (Fig. 8) and the experimental crack initiation sites, which vary between $\Psi = 90°$ and $\Psi = 135°$ [1–3] (see Table 1).

Comparison of experimental fatigue results and fatigue lifetime estimations

The experimental fatigue results presented in Table 1, originally in terms of the applied load range (ΔF), were re-evaluated in terms of the equivalent von Mises stress range. This was achieved using the following approaches:

- the FEMFAT *Shell* WELD approach combined with *Eurocode 3/9* analysis method (see Fig. 5).
- the FEMFAT *Shell* WELD approach combined with *ECS standard* analysis method (see Fig. 6).
- the FEMFAT *Solid*WELD approach combined with *ECS standard* analysis method (see Fig. 7).
- the FEMFAT R1MS approach combined with the *ECS standard* analysis method (see Fig. 8).

A dedicated *stress amplitude* scale factor was calculated for each data point in Table 1. For each FE model analysed, the stress amplitude data imported from Ansys was multiplied by the relevant *stress amplitude scale factor* to account for the actual load amplitude applied in the experimental tests and the effect of corrosion in sea-water.

$$f_s = \frac{1}{f_c} \cdot \frac{\Delta F_{\text{exp,max}}}{2 \cdot F_{\text{FEA}}} \qquad \textit{Equation (2)}$$

In the above expression:

- $\Delta F_{exp.max}$ represents the maximum load range applied in the experimental fatigue test.
- F_{FEA} is the amplitude of the load applied in the FE analysis performed in Ansys Mechanical (*i.e.* $F = 1\ MN$; see Fig. 3).
- f_c = 0.7 considers the impact of corrosion, as outlined in GL 2007 [5].

It is worth noting that sea-water corrosion generally reduces the fatigue strength of welded joints. Consequently, the fatigue limit of the S-N design curve used for the fatigue strength assessment must be multiplied by the f_c factor, as described in reference [5]. This ultimately reduces the fatigue strength by 30%. However, the FEMFAT software does not currently incorporate an *Influence Factor* to account for corrosion's effect on the fatigue limit of the presented S-N curves. To address this issue, the f_c factor was incorporated into the stress *amplitude scale factor* (f_s). This allows the experimental fatigue data to be corrected prior to fatigue analysis, without modifying the S-N curves employed by FEMFAT in its calculations.

Figs. 9–12 show a comparison of the re-evaluated experimental data with the S-N design curves for steel welded joints as adopted by FEMFAT for each of the four analysis approaches considered (see Table 4). The reported markers relate to the experimental data in terms of

- the number of cycles to crack initiation (N_{init})
- the number of cycles to breakthrough (i.e. when a through-the-thickness crack occurs at the weld toe on the chord side (N_{bt})).

For each approach in Table 4 and each specimen in Table 1, the number of cycles predicted by FEMFAT can be determined by horizontally intersecting the relevant S-N design curve (PS 50% or PS 97.7%) with the given $\Delta\sigma_{eq,vM}$ value, as shown in Figs. 9–12. Accordingly, results to the left of the PS 50% S-N design curve indicate that crack initiation occurred in the experiments, before the estimated fatigue failure. These results are therefore considered unsafe.

FEMFAT approach	FEMFAT WELD method	Slope k	Slope k'	$\Delta\sigma_D$ (PS50%) [MPa]	N_D [cycles]
***Shell* WELD**	*(a) Eurocode 3/9*	3.0	5.0	269.4	$5.00 \cdot 10^6$
***Shell* WELD**	*(b) FEMFAT 4.7*	4.0	7.0	442	$1.00 \cdot 10^6$
***Solid*WELD**	*(c) FEMFAT 4.7*	3.1	5.2	262	$2.00 \cdot 10^6$
R1MS	*(d) FEMFAT 4.7*	5.0	5.0	220	$1.80 \cdot 10^6$

Table 4. Summary of the S-N fatigue design curves implemented by FEMFAT (also see Figs. 9–12).

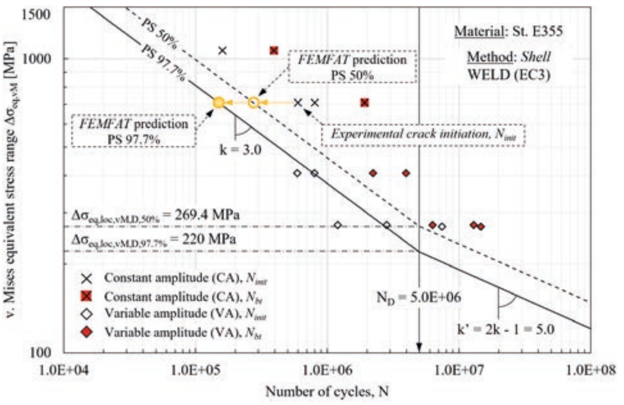

Fig. 9. Fatigue strength assessment of welded K-nodes using the FEMFAT Shell WELD approach in conjunction with the Eurocode 3 analysis method. The fatigue design curve for welded steel joints, as defined by Eurocode 3 and recorded in the FEMFAT database, was compared with experimental fatigue data obtained from constant and variable amplitude fatigue tests (see references [1–3]).

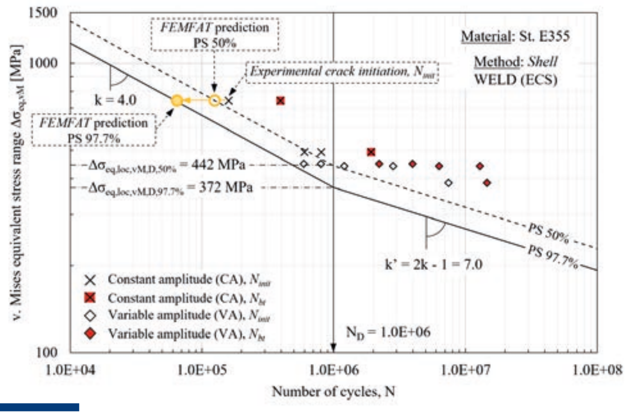

Fig. 10. Fatigue strength assessment of welded K-nodes using the FEMFAT Shell WELD approach in combination with the FEMFAT 4.7 analysis method. The fatigue design curve for welded steel joints, as defined by the ECS standard in the FEMFAT database, was compared with the experimental fatigue data from constant and variable amplitude fatigue tests referenced in [1–3].

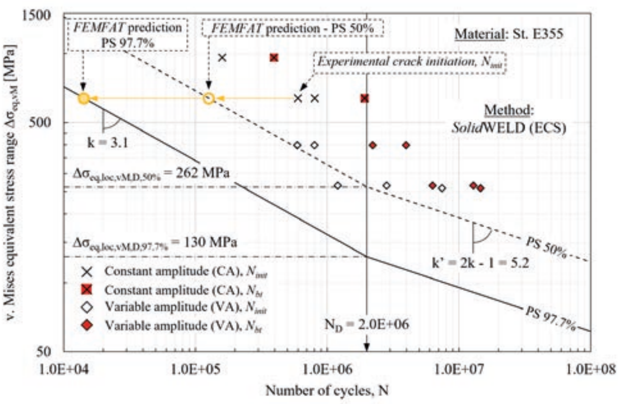

Fig. 11. Fatigue strength assessment of welded K-nodes using the FEMFAT SolidWELD approach and the FEMFAT 4.7 analysis method. It compares the fatigue design curve for welded steel joints as defined by the ECS standard in the FEMFAT database and with experimental fatigue data from constant and variable amplitude fatigue tests referenced in [1–3].

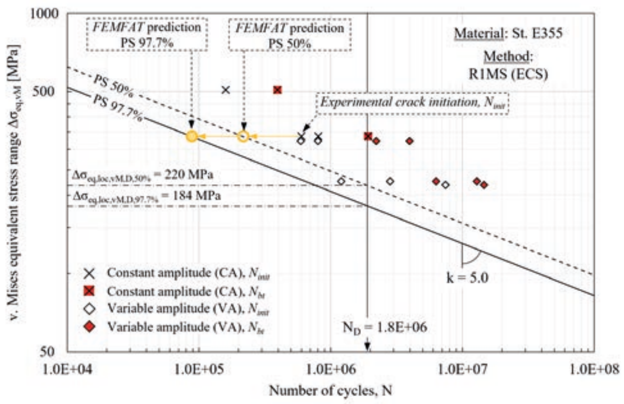

Fig. 12. Fatigue strength assessment of welded K-nodes using the FEMFAT R1MS approach together with the FEMFAT 4.7 analysis method. The fatigue design curve for welded steel joints, as defined by the ECS standard in the FEMFAT database, is compared with the experimental fatigue data from constant and variable amplitude fatigue tests referenced in [1–3].

Conversely, results to the right of the PS 50% S-N design curve are considered safe, indicating that the actual crack initiation during the experiment occurred after the estimated fatigue lifetime. Finally, Table 5 summarizes the comparison between the experimental results and FEMFAT's predictions in terms of the number of cycles to crack initiation at 50% and 97.7% probability of survival.

Fig. 9 shows a comparison of the fatigue design curve for steel welded joints as defined by Eurocode 3, with experimental fatigue data obtained from constant and variable amplitude fatigue tests referenced in [1–3]. This data was then re-evaluated in terms of the von Mises equivalent stress range calculated at the most critical point using the FEMFAT *Shell* WELD approach in conjunction with the *Eurocode 3/9* analysis method (see Fig. 5).

The S-N curve is defined by a slope $k = 3$ and a fatigue limit of $\Delta\sigma_D = 269.4MPa$ (PS 50%) at $N_D = 5{\cdot}10^6$ cycles. According to the *Miner Modified* formulation (see Table 3), a slope of $k' = 2k\text{-}1 = 5$ is adopted for $N > N_D$ (see Table 4). Table 5 compares the number of cycles to crack initiation in the experiments with the estimated fatigue life using the aforementioned FEMFAT S-N design curve and 50% probability of survival for each specimen. In the case of CA loads and a 50% probability of survival, all three of the experimental results relating to crack initiation are considered safe. Conversely, with VA loads and a 50% probability of survival, only one of the five crack initiation experiment results is deemed safe. Ultimately, all CA and VA results relevant to the break-through lie within the safe zone of the S-N design curve.

Fig. 10 shows a comparison of the fatigue design curve for steel welded joints, as defined by the ECS standard in the FEMFAT database, and re-evaluated experimental fatigue data from constant and variable amplitude fatigue tests from [1–3] in terms of the von Mises equivalent stress range. The von Mises equivalent stress range was calculated at the most critical point using the FEMFAT *Shell* WELD approach in conjunction with the *FEMFAT 4.7* analysis method (see Fig. 6).

The local S-N curve at the most critical node is defined by a slope $k = 4$ and a fatigue strength limit of $\Delta\sigma_D = 442MPa$ (PS 50%) at $N_D = 1{\cdot}10^6$ cycles. According to the *Miner Modified* formulation (see Table 3), a slope $k' = 2k\text{-}1 = 7$ is adopted for $N > N_D$ (see Table 4). Table 5 shows a comparison of the number of cycles to crack initiation in experiments with the estimated fatigue life using the proposed FEMFAT S-N design curve, given a 50% probability of survival.

Specimen No.	Crack initiation Experimental results	FEMFAT prediction Shell WELD (EC3) Fig. 9		FEMFAT prediction Shell WELD (ECS) Fig. 10		FEMFAT prediction *Solid*WELD (ECS) Fig. 11		FEMFAT prediction R1MS (ECS) Fig. 12	
		$N_{predicted}$ [cycles]		$N_{predicted}$ [cycles]		$N_{predicted}$ [cycles]		$N_{predicted}$ [cycles]	
	N_{init} [cycles]	PS 50%	PS 97.7%	PS 50%	PS 97.7%	PS 50%	PS 97.7%	PS 50%	PS 97.7%
6, CA	$1.60 \cdot 10^5$	$8.00 \cdot 10^4$	$4.36 \cdot 10^4$	$1.25 \cdot 10^5$	$6.29 \cdot 10^4$	$3.55 \cdot 10^4$	$4.05 \cdot 10^3$	$2.75 \cdot 10^4$	$1.13 \cdot 10^4$
7a, CA	$6.00 \cdot 10^5$	$2.74 \cdot 10^5$	$1.49 \cdot 10^5$	$6.47 \cdot 10^5$	$3.25 \cdot 10^5$	$1.27 \cdot 10^5$	$1.44 \cdot 10^4$	$2.14 \cdot 10^5$	$8.76 \cdot 10^4$
7b, CA	$8.05 \cdot 10^5$	$2.74 \cdot 10^5$	$1.49 \cdot 10^5$	$6.47 \cdot 10^5$	$3.25 \cdot 10^5$	$1.27 \cdot 10^5$	$1.44 \cdot 10^4$	$2.14 \cdot 10^5$	$8.76 \cdot 10^4$
1, VA	$5.93 \cdot 10^5$	$1.44 \cdot 10^6$	$7.83 \cdot 10^5$	$9.39 \cdot 10^5$	$4.71 \cdot 10^5$	$5.48 \cdot 10^5$	$6.24 \cdot 10^4$	$2.64 \cdot 10^5$	$1.08 \cdot 10^4$
10, VA	$8.00 \cdot 10^5$	$1.44 \cdot 10^6$	$7.83 \cdot 10^5$	$9.39 \cdot 10^5$	$4.71 \cdot 10^5$	$5.48 \cdot 10^5$	$6.24 \cdot 10^4$	$2.64 \cdot 10^5$	$1.08 \cdot 10^4$
13, VA	$7.42 \cdot 10^5$	$5.04 \cdot 10^6$	$2.75 \cdot 10^6$	$1.71 \cdot 10^6$	$8.57 \cdot 10^5$	$2.08 \cdot 10^6$	$2.37 \cdot 10^5$	$1.85 \cdot 10^6$	$7.59 \cdot 10^5$
3, VA	$2.82 \cdot 10^6$	$4.86 \cdot 10^6$	$2.65 \cdot 10^6$	$1.01 \cdot 10^6$	$5.05 \cdot 10^5$	$1.93 \cdot 10^6$	$2.19 \cdot 10^5$	$1.57 \cdot 10^6$	$6.42 \cdot 10^5$
2, VA	$1.20 \cdot 10^6$	$4.86 \cdot 10^6$	$2.65 \cdot 10^6$	$1.01 \cdot 10^6$	$5.05 \cdot 10^5$	$1.93 \cdot 10^6$	$2.19 \cdot 10^5$	$1.57 \cdot 10^6$	$6.42 \cdot 10^5$

Table 5. Overall comparison of the experimental results in terms of number of cycles to crack initiation with the numerical estimations using the S-N fatigue design curves implemented in FEMFAT (see Table 4).

For CA loads and a 50% probability of survival, two out of three experimental results relevant to crack initiation are considered safe, while one is considered unsafe. Conversely, for VA loads and a 50% probability of survival, three out of five experimental results relevant to crack initiation are considered safe, while two are considered unsafe. Overall, all CA and VA results relevant to the break-through lie on the safe side of the S-N design curve.

Fig. 11 shows a comparison of the fatigue design curves for steel welded joints as defined by the ECS standard in the FEMFAT database with experimental fatigue data obtained from constant and variable amplitude fatigue tests as reported in references [1–3]. This data was re-evaluated in terms of the von Mises equivalent stress range calculated at the most critical point, according to the FEMFAT *Solid*WELD approach combined with the *FEMFAT 4.7* analysis method (see Fig. 7).

The local S-N curve at the most critical node is defined by a slope $k = 3.1$ and endurance fatigue limit of $\Delta\sigma_D = 262MPa$ (PS 50%) at $N_D = 2{\cdot}10^6$ cycles. According to the *Miner Modified* formulation (see Table 3), a slope of $k' = 2k\text{-}1 = 5.2$ is adopted for $N > N_D$ (see Table 4). Table 5 compares the number of cycles to crack initiation in experiments with fatigue life estimates obtained using the previously described FEMFAT S-N design curve for a 50% probability of survival.

For CA loads and a 50% probability of survival, all three experimental crack initiation results fall within the safe range. For VA loads and a 50% probability of survival, four out of five crack initiation results in the experiments fall within the safe range, while one result lies within the unsafe range of the S-N curve (PS 50%). In the break-through conditions, all three CA results and all five VA results lie in the safe range of the S-N design curve.

Finally, Fig. 12 shows a comparison of the fatigue design curve for welded steel joints as defined by the ECS standard in the FEMFAT database, alongside experimental fatigue data obtained from constant and variable amplitude fatigue tests (see references [1–3]). This data was re-evaluated in terms of the von Mises equivalent stress range, calculated at the most critical point using the FEMFAT R1MS approach combined with the *FEMFAT 4.7* analysis method (see Fig. 8).

The local S-N curve at the most critical node is defined by a slope of $k = 5.0$ and a fatigue limit strength of $\Delta\sigma_D = 220MPa$ (PS 50%) at $N_D = 1.80{\cdot}10^6$ cycles. According to the Miner Elementary formulation (see Table 3), the same slope $k' = k = 5.0$ is used for $N > N_D$ (see Table 4). Table 5 compares the fatigue life predicted using the FEMFAT S-N design curve for the R1MS approach with the number of cycles to crack initiation observed in experiments on each specimen. For CA loads and a 50% probability of survival, all three experimental crack initiation results lie within the safe range. For VA loads and a 50% probability of survival, four out of five experimental results crack initiation results lie within the safe range, while one result lies outside this range. Ultimately, all CA and VA results relevant to the break-through are on the safe side of the S-N design curve.

Conclusions

The fatigue strength of large welded K-nodes in E355 structural steel was investigated numerically using the MAGNA FEMFAT commercial fatigue analysis software. According to the FEMFAT guidelines, four different fatigue strength assessment approaches were implemented in FEMFAT using three different FE model combinations created in Ansys Mechanical:

- the *Shell* WELD approach combined with the *Eurocode 3/9* analysis method,
- the *Shell* WELD approach combined with the *FEMFAT 4.7* analysis method,
- the *Solid*WELD approach combined with the *FEMFAT 4.7* analysis method, and
- the R1MS approach combined with the *FEMFAT 4.7* analysis method.

A set of experimental fatigue data relating to the geometry of the welded K-node under investigation, taken from the literature, was re-evaluated in terms of the von Mises equivalent stress range. These were then compared with the S-N fatigue design curves implemented by the FEMFAT software.

The automated analysis procedure implemented by FEMFAT enabled the fatigue strength of the welded connections between the brace and chord to be assessed using input FE models solved in Ansys Mechanical. Thanks to the meshing rules provided in the FEMFAT guidelines, a coarse global mesh was adopted for the shell input model. A locally refined mesh was required for the solid input model near the welds. However, a coarser mesh was used further away, significantly reducing the computational effort required for the FE analysis.

The FEMFAT tool enables users to:

- easily import FE mesh entities and relevant stress results for each input model.
- automatically identify *weld edges* in the case of the *shell* input model and assign suitable joint details for weld nodes based on the FEMFAT WELD databases.
- import a time-history of applied CA or VA loads;
- define the material properties;
- select the desired analysis method for assessing the fatigue strength of the welds according to *Eurocode 3/9* and *FEMFAT 4.7*.
- select the equivalent stress formulation to be used e.g. the von Mises equivalent stress; and
- select the damage calculation according to the Miner rule, e.g. *Miner Modified* and *Miner Elementary.*

All the approaches considered and described by FEMFAT successfully identified the most critical point of the welded connection between the brace tube and the chord tube in the saddle point region ($90° < \Psi < 125°$ in the least conservative case), in accordance with experimental fatigue crack evidence ($90° < \Psi < 135°$).

About the University of Padua's Department of Industrial Engineering (DII)

The Department of Industrial Engineering (DII) at the University of Padua is a centre of excellence for research and training in various engineering disciplines, including aerospace, chemical, electrical, energy, materials, and mechanical engineering. The department's mission is to promote innovation and competitiveness in industrial engineering through excellence in research and training.

Since its establishment in 2012 through the merger of six independent departments, the DII has grown to include 48 research laboratories and now offers four undergraduate (First Level) degrees, seven post-graduate (Second Level) degrees, two doctoral programs, and a variety of master's courses. The department employs over 500 people, including professors, researchers, doctoral students, and technical and administrative staff.

Around 50% of revenue is derived from collaborations with industries and research centres. The numerous spin-off companies demonstrate the DII's entrepreneurial spirit.

There was good agreement between the experimental crack initiation results and the proposed S-N curves when the FEMFAT *Shell* WELD approach was combined with the *Eurocode 3/9* and *FEMFAT 4.7* analysis methods.

The experimental data was distributed around the S-N design curve for a 50% probability of survival. For the FEMFAT *Solid*WELD approach, the experimental crack initiation data was mostly consistent with the PS 50% design curve. Besides the *Shell* WELD and the *Solid*WELD approaches, the R1MS approach was also used and provided safe estimates with respect to the experimental crack initiation data.

All of the fatigue strength assessment approaches considered provided safe fatigue durability estimates for the experimental data at break-through in relation to the PS 50% S-N curves. The FEMFAT fatigue analysis tool ultimately enabled the rapid evaluation of the large-scale K-node joint via the *Shell* WELD approach, thanks to the option of using a coarse mesh in the input FE model. Solving the FEMFAT *Shell* WELD analyses took less than five seconds for the CA loads and less than five minutes for the VA loads.

The *Solid*WELD approach required a longer solution time because a FE mesh with a 1mm refinement was needed at the weld toes. This equated to 60 seconds for CA loads and 60 minutes for VA loads. Ultimately, solving the R1MS analysis took up to 20 hours for VA loads, producing fatigue strength estimates comparable to those of the *Shell* WELD and *Solid*WELD approaches.

Using FEMFAT alongside the coarse mesh shell input models according to the *Shell* WELD method, significantly reduced the computational resources required to analyse the welded K-node, compared to the resources needed for the fatigue analysis using the complete *solid* model according to the *Solid*WELD approach.

For more information:
Professor Giovanni Meneghetti – University of Padova
giovanni.meneghetti@unipd.it

References

[1] D. Radaj, C. M. Sonsino, and W. Fricke, *Fatigue assessment of welded joints by local approaches,* Woodhead Publishing: Sawston, United Kingdom, 2006. HYPERLINK: doi.org/10.1533/9781845691882

[2] C. M. Sonsino, "Structural Durability Assessment of Welded Offshore K-Nodes by Different Local Design Concepts", *Frattura ed Integrità Strutturale*, vol. 3 (9), pp. 3–12, Jul. 2009, HYPERLINK: doi.org/10.3221/IGF-ESIS.09.01

[3] C. M. Sonsino, "Comparison of different local design concepts for the structural durability assessment of welded offshore K-nodes", *International Journal of Fatigue*, vol. 34, pp. 27–34, Jan. 2012, doi.org/10.1016/j.ijfatigue.2010.09.005

[4] *Magna Powertrain FEMFAT 2024 WELD User Manual*, MAGNA Powertrain, St. Valentin, Austria, 2024

[5] *GL Rules for Classification and Construction*, IV: Industrial Services, Part 6: Offshore Technology, Section 4: Structural Design, Germanischer Lloyd Aktiengesellschaft, Hamburg, Germany, 2007.